CRYSTAL GROWTH & DESIGN
2002
VOL. 2, NO. 5
363−370

Delivered at the Crystal Engineering to Crystal Growth: Design and Function Symposium, ACS 223rd National Meeting, Orlando, Florida, April 7−11, 2002

Paracetamol Crystallization Using Laser Backscattering and ATR-FTIR Spectroscopy: Metastability, Agglomeration, and Control

Mitsuko Fujiwara, Pui Shan Chow, David L. Ma, and Richard D. Braatz*

School of Chemical Sciences, 600 South Mathews Avenue, Box C-3, University of Illinois at Urbana-Champaign, Urbana, Illinois 61801

Received April 1, 2002

ABSTRACT: A systematic approach is developed for the in situ control of the crystal size distribution, and is applied to the aqueous crystallization of paracetamol (acetaminophen) as a model pharmaceutical system. This involves the determination of the solubility curve and the metastable limit, and the operation of concentration-controlled batch crystallization. The solution concentration and the solubility curve of paracetamol in water are determined using attenuated total reflection (ATR)-Fourier transform infrared (FTIR) spectroscopy coupled with chemometrics. The metastable zone width of paracetamol is determined using laser backscattering and ATR-FTIR spectroscopy. Seeded batch crystallizations of paracetamol following a desired supersaturation profile near the metastable limit are carried out using in situ solution concentration measurements obtained from ATR-FTIR spectroscopy. The in situ chord length distributions of crystals obtained from laser backscattering are related to characteristics of the crystal size distribution. Product crystals where the supersaturation temporarily exceeded the metastable limit during operation contained agglomerates and exhibited large size variation. Larger product crystals of more uniform size and shape are obtained from operation where supersaturation was successfully controlled to stay within the metastable limit.

1. Introduction

Most pharmaceutical manufacturing processes include a series of crystallization processes from solution to achieve high purity and to produce the desired final crystal form. The operating conditions of the crystallization process determine the physical properties of the products such as the crystal purity, size, and shape distribution. This study considers the crystallization of paracetamol (acetaminophen, *p*-hydroxyacetanilide) from aqueous solution. Paracetamol is a widely used analgesic (pain relief) and antipyretic (fever reducer). It is the active ingredient in over-the-counter products such as Tylenol and is used as an alternative to aspirin. Paracetamol is often used as a model pharmaceutical for crystallization studies.[1,2] Previous studies measured the growth rates of different faces of paracetamol crystals[3−5] and determined the growth kinetics.[6] Previous nucleation studies examined the effects of additives and solvents on paracetamol nucleation carried out isothermally.[6−10]

In this work, paracetamol in water was selected as the model system because of its low solubility and its tendency to form agglomerates during crystallization. The low solubility makes it especially challenging to measure the characteristics of the particle size distribution due to the low number of crystals formed during crystallization, and to measure the solution concentration with high enough accuracy for characterizing the kinetics or for on-line control of batch crystallization. Agglomeration is a common problem in the crystallization of pharmaceuticals, which can lead to solvent inclusions that can reduce the shelf life of the drug. Interpreting size distribution measurements from particle size analyzers is more difficult for agglomerating systems. Our goal is to operate the crystallizer in such a way that agglomeration is avoided, and large paracetamol crystals are formed.

When optimizing the size and shape of the crystals during batch crystallization, it is often preferred to operate within the metastable zone to avoid undesired nucleation.[11] Hence determining the metastable zone is typically the first step in designing a crystallization process for the production of reproducible crystals. The lower bound on the metastable zone is the solubility curve. Numerous methods are available for measuring the solution concentration,[12,13] which can be used to construct solubility curves. Here we use ATR-FTIR spectroscopy, in which the in situ probe inserted directly into the slurry allows measurement of the infrared spectrum of the solution.[14−21] Advantages of ATR-FTIR spectroscopy over other on-line measurement systems, such as conductivity or densitometry, include its applicability to organic systems, its ability to measure multiple solution concentrations in multicomponent

* Corresponding author: 217-333-5073 (phone), 217-333-5052 (fax), braatz@uiuc.edu (email).

10.1021/cg0200098 CCC: $22.00
Published on Web 08/10/2002

systems, and its avoidance of an external sampling loop, which can cause operating problems.[18,22]

The upper bound on the metastable zone, which is the metastable limit, is dependent on various factors including the cooling rate, impurities, and mixing speed.[23] There are various methods for detecting the spontaneous nucleation that occurs at the metastable limit. Common methods are observation by the naked eye to detect the onset of cloudiness of solution and optical density changes detected by light transmission. Laser backscattering measures in situ the characteristics of the crystal size distribution. It has been used to monitor nucleation and dissolution during crystallization[24] and provides an alternate method of detecting nucleation associated with the metastable limit.[25] ATR-FTIR spectroscopy has been used to determine the metastable limit by measuring the reduction in solution concentration associated with the onset of nucleation.[15,17,18] Here the three methods for detecting the onset of nucleation: naked eye, laser backscattering, and ATR-FTIR spectroscopy, are compared for the detection of metastable limit of paracetamol in water.

The metastable zone specifies the operating conditions for the design of experiments for the determination of secondary nucleation and growth kinetics,[26,27] and specifies the default conditions for operating an industrial crystallization process. In batch crystallization, usually the feedback controller is designed to follow a temperature profile[12,28] rather than a supersaturation profile[29] because of the ease of measuring the temperature compared to supersaturation. Rigorous determination of an optimal temperature profile requires accurate growth and nucleation kinetics, which can be determined in a series of continuous or batch experiments. For agglomerating and other complex crystallization systems, it may be difficult to determine kinetics that are accurate enough to obtain an optimal temperature profile. An alternative approach that does not require accurate kinetics is to control the crystallizer so that it follows a supersaturation profile in the metastable zone. The profile would be located to trade off the desire for fast growth rates which occur near the metastable limit with low nucleation rates which occur near the solubility curve. The implementation of ATR-FTIR spectroscopy with appropriate data analysis enables in situ measurement of solution concentration that overcomes the aforementioned drawbacks associated with on-line solution concentration measurement. In this paper, a control scheme for batch crystallization following a supersaturation profile using ATR-FTIR spectroscopy is described, and the results from the operation of seeded batch crystallization of paracetamol near the metastable limit are presented. The supersaturation profile was chosen to maximize the growth rate subject to the constraint of having negligible nucleation.

2. Experimental Procedure

2.1 Materials and Instruments. Aqueous paracetamol spectra were obtained by a DIPPER-210 ATR immersion probe with two reflections manufactured by Axiom Analytical. ZnSe was used as the internal reflectance element. The probe was attached to a Nicolet Protege 460 FTIR spectrophotometer connected to a Pentium II computer running OMNIC 4.1a software from Nicolet Instrument Corp. The spectrometer was purged with N_2 gas 2 h before and while measurements were being taken to reduce the effects of CO_2 absorption in its optical path. A spectral resolution of 4 cm^{-1} was used. Degassed deionized water at room temperature was used for the background measurement. Care was taken to minimize air bubbles on the ATR probe tip as bubbles covering the crystal surface would reduce the absorbance. Chord length distributions of paracetamol crystals in solution were obtained using Lasentec focused beam reflectance measurement (FBRM) connected to a Pentium III running version 6.0b9 of FBRM Control Interface software. The sample temperature was controlled by ratioing the hot and cold water to the jacket with a research control valve (Badger Meter, Inc.) using a proportional-integral control system designed via internal model control[30,31]and was measured every 2 s using a Teflon-coated thermocouple attached to a Data Translation 3004 data acquisition board via a Fluke 80TK thermocouple module. Temperature readings were averaged during the collection of each FTIR spectra, which consisted of 32 scans (approximately 20 s). The same instrument conditions were used for all experiments.

Table 1: Paracetamol−Water Solutions Used for Calibration

concentration (g/g of water)	temperature range (°C)
0.00998	33−18
0.0145	38−23
0.0199	43−29
0.0250	48−36
0.0300	53−41
0.0349	58−46

2.2 Calibration for Solution Concentration. Specified amounts of paracetamol (4-acetamidophenol, 98%, melting point 167 °C) obtained from Aldrich and degassed deionized water were placed in a 500 mL jacketed round-bottom flask and heated until all crystals dissolved. Samples were stirred using a magnetic stirrer. Each solution was cooled at 0.5 °C/min while spectral data were collected every minute in the range between 650 and 4000 cm^{-1} for a span of 15 °C or until crystals started to appear. The IR spectra were collected for six different solution concentrations (see Table 1).

The IR spectra measured using the ATR-FTIR probe are a function of the solution concentration and temperature of the samples. Several calibration schemes are available to estimate the solution concentration from the IR spectra.[15−18,20] The most accurate calibrations incorporate absorbances in a range of frequencies, as opposed to a peak absorbance or the area under a peak, to construct a calibration model which relates the IR spectra to the solution concentration. Such calibrations can be calculated using *chemometrics*,[32−34] which is a class of multivariable statistical algorithms. A robust chemometrics procedure[20,21] constructs calibration models using a variety of chemometric techniques (such as principal component regression and partial least squares), and then selects the model that produces the most accurate predictions (smallest prediction intervals). This procedure, implemented with MATLAB 5.3 (The MathWorks, Inc.), was used to construct a linear calibration model between the solution concentration and the slurry temperature and absorbances of the IR spectra. The assumption of linearity was confirmed as described previously.[20] Using IR absorbances in frequency 1100−1800 cm^{-1}, calibration models were constructed using six different chemometrics methods, with correlation principal component regression (CPCR)[36] producing the smallest prediction intervals. A noise level of 0.001 was used in the chemometrics method since it resulted in prediction intervals consistent with the accuracy of the solubility data (0.00014 g/g of solvent). The resulting calibration model is

$$C = \sum_{i=1100}^{1800} w_i a_i + w_T T + w_o \qquad (1)$$

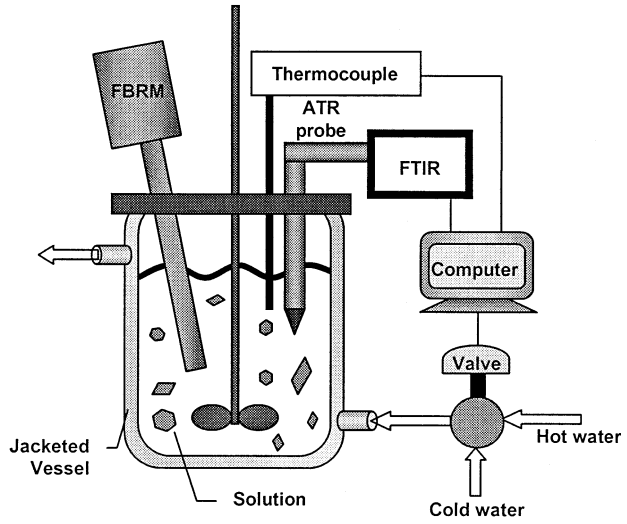

Figure 1. Batch crystallizer schematic for supersaturation control (not drawn to scale).

where C is the concentration, a_i is the absorbance at frequency i cm^{-1}, T is the temperature, and w_i, w_T, and w_o are regression coefficients.

2.3 Solubility Determination. To determine the solubility curve, ATR-FTIR spectra for paracetamol slurry were recorded at temperatures ranging from 20 to 50 °C. The slurry was equilibrated at each temperature for about an hour. Five scans were collected at each temperature, which was approached from both undersaturation and supersaturation to ensure that the slurry had reached equilibrium, resulting in 10 total spectra per temperature setting. The solution concentration of paracetamol was calculated from each spectra using the calibration model obtained above.

2.4 Metastable Zone Measurements. The metastable zone width of paracetamol solution was determined by the polythermal method.[23] Paracetamol solution of various concentrations was prepared in a 500-mL jacketed round-bottom flask. The solution was heated to about 5 °C above its saturation temperature for about 1 h and then cooled at 3.7 °C/h until visible crystals appeared. The solution concentration was measured from ATR-FTIR spectra using the aforementioned calibration model, and the chord length distributions of the crystals were measured using FBRM with 10 s measurement duration while the solution was observed with the naked eye for the formation of crystals. The metastable limit for cooling rate of 30 °C/h was detected by eye during the calibration experiments (described above) and from experiments carried out similarly.

2.5 Seeded Batch Crystallization. An appropriate amount of paracetamol in 350 g of water was heated to its saturation temperature in a 500-mL jacketed round-bottom flask while stirring at 350 rpm using an overhead mixer until all crystals dissolved. The crystallizer was cooled to a temperature in the middle of the metastable zone, and 0.5 g of dry seed crystals were added. The crystallizer jacket water flow was controlled using a proportional-integral control system designed via internal model control[30,31] to follow a preset supersaturation curve ($C_{set} = 4.754 \times 10^{-7}T^3 - 3.409 \times 10^{-5}T^2 + 1.296 \times 10^{-3}T - 1.242 \times 10^{-3}$) close to the metastable limit based on solution concentration measurements obtained from ATR-FTIR spectra coupled with aforementioned calibration model. The chord length distribution was measured every minute during operation using FBRM. The schematic of the batch crystallization apparatus for supersaturation control is shown in Figure 1. Seed crystals were prepared by batch cooling crystallization as described previously.[6] Sieve fractions (125−250 μm for run 1 and 250−345 μm for run 2) were used directly as seeds.

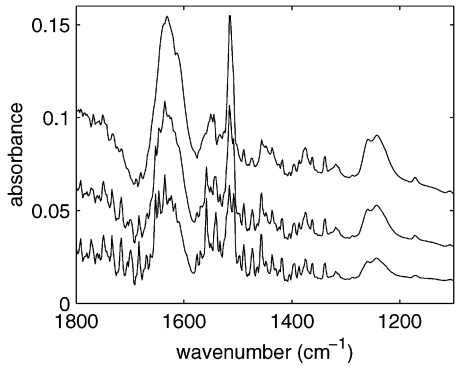

Figure 2. Representative ATR-FTIR spectra of aqueous paracetamol solutions used for calibration listed in Table 1. The spectra are in ascending order from low to high concentration (0.0145 g/g at 38 °C, 0.0250 g/g at 48 °C, and 0.0349 g/g at 58 °C).

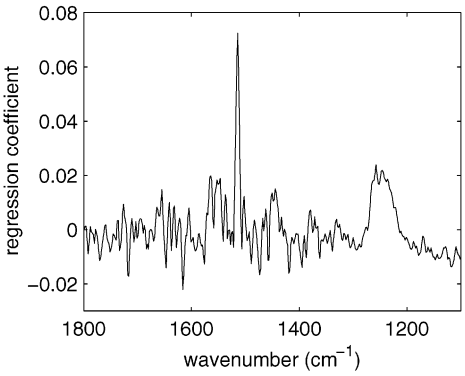

Figure 3. Regression coefficients for calibration model which relates ATR-FTIR spectra to solution concentration. The regression coefficients for the temperature and the intercept are not shown.

3. Results and Discussion

3.1 Calibration Model. The spectra of aqueous paracetamol solution in the range 1100−1800 cm^{-1} (Figure 2) were used to build a calibration model which relates the IR spectra to solution concentration. The absorbance in this region increased with concentration and temperature. The IR peak assignments of paracetamol in aqueous solution at room temperature are given previously.[35] Because of the low solubility of paracetamol in water, the contribution of noise becomes significant and obtaining an accurate solution concentration measurement is challenging. Hence an advanced chemometric approach was used since it can produce calibration models that are an order-of-magnitude more accurate than methods based on absorbances at peaks.[20,21] The regression coefficients for the calibration model (see Figure 3) show a broad peak at 1250 cm^{-1}, indicating that the absorbances at these frequencies show a consistent positive correlation with the concentration of paracetamol in aqueous solution. This should not be surprising since this portion of the spectra is the least noisy (see Figure 2). There is a high positive correlation between the solution concentration and the absorbance at 1514 cm^{-1}. The correlations between the solution concentration and the absorbances in the broad peak at 1575 cm^{-1} (see Figure 2) are much smaller than for the peaks at 1514 and 1250 cm^{-1}. A significant advantage of using chemometrics to construct the

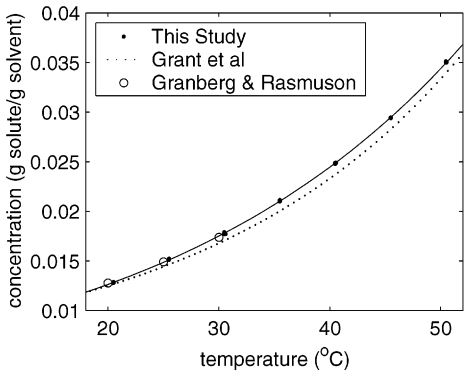

Figure 4. Solubility curve of paracetamol in water obtained from ATR-FTIR spectroscopy and chemometrics. The data are fit to $\ln C_o = 5193.109T^{-1} + 27.121124 \ln T - 178.28055$. The solubility curve is compared to previously published data.[37,38]

calibration model is its ability to automatically factor in the relative signal-to-noise ratios as well as the magnitude of the absorbances, and its ability to average the effect of noise over many absorbances.

3.2 Solubility Curve. The solubility of paracetamol in water in the temperature range from 20 to 50 °C was determined from ATR-FTIR spectra using the aforementioned calibration model. The data were fit to

$$\ln C_o = -(a/R)T^{-1} + (b/R)\ln T + c \qquad (2)$$

where R is the ideal gas constant, T is in units of Kelvin, and C_o is in units of mole fraction[37] (see Figure 4). The solubility is in reasonably good agreement (within 0.0012 g/g of solvent) with Grant et al.[37] The difference in solubility can be attributed to differences in the purity of paracetamol and water used. For 20−30 °C, where data can be compared, the solubility is in better agreement with Granberg and Rasmuson[38] (within 0.00014 g/g of solvent, which is statistically insignificant since it is less than the prediction ability of the calibration model). From the coefficients of the solubility curve, the apparent enthalpy of solution,[37] $\Delta H^* = a + bT$, of paracetamol was calculated to be 24.05 kJ/mol at 298.15 K, and the apparent heat capacity of paracetamol, $C_p^* = b = 225.5$ J/mol K. Although the coefficients of the solubility curve are different, the calculated enthalpy of solution is in reasonable agreement with Grant et al. (21.7 kJ/mol).[37]

3.3 Metastable Zone Determination. The metastable zone is a region where the solution is supersaturated while spontaneous crystallization does not occur. In the polythermal method,[23] a saturated solution at slightly above its saturation temperature is cooled at a constant rate until spontaneous nucleation is visible at the metastable limit. The metastable limit of paracetamol at cooling rates of 3.7 °C/h (slow cool) and 30 °C/h (fast cool) were determined. The metastable zone for the faster cooling rate is wider than for the slower cooling rate as shown in Figure 5.

While cooling in the metastable zone, the supersaturation and the number of nuclei both increase; however, the nuclei are not visible since they are in the subnanometer range. The nuclei have to grow to a certain size to be detectable, and the solution remains clear until the detectable size is reached at the metastable limit. Three methods were compared in determining the

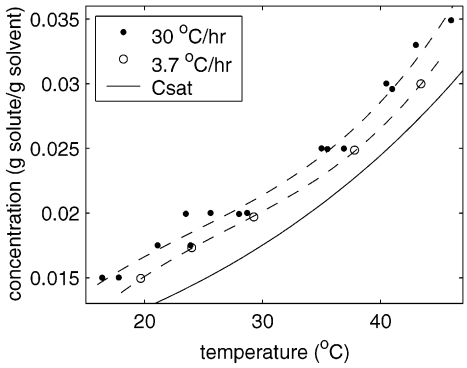

Figure 5. Metastable limit of paracetamol solution for cooling rates of 30 °C/h (•) and 3.7 °C/h (○) is plotted with solubility curve (—). Third-order polynomials fit to each data set using least-squares (- -) are shown.

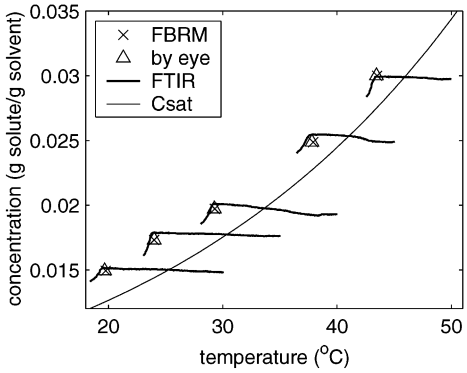

Figure 6. Metastable limit of paracetamol solution at a cooling rate of 3.7 °C/h detected by FBRM (×), by eye (△), and by ATR-FTIR spectroscopy (—) plotted with solubility curve (- -).

metastable limit for the slow cooling rate: (i) direct visual observation for occurrence of cloudiness in the solution, (ii) change in the solution concentration as measured by ATR-FTIR spectroscopy, and (iii) change in the chord length distribution as measured by laser backscattering (see Figure 6). ATR-FTIR data indicate that the solution concentration is nearly constant inside the metastable zone and the supersaturation significantly decreases past the metastable limit.

The chord length distribution was measured using laser backscattering (FBRM) to detect the onset of nucleation. The chord length distribution is reported as the number of "counts" (particle size measurements collected within FBRM sampling time) within each size range (e.g., 2−4 μm). The "total counts" sums the counts in all the size ranges. The FBRM software includes various weighted distributions, which emphasize different size ranges. For example, the 1/length weighting divides the number of counts in each size range by the midpoint of the size range, so that small particles are emphasized. The square weighting multiplies the number of counts in each size range by the square of the midpoint of the size range, which emphasizes larger particles in the distribution. These built-in statistics for FBRM were evaluated to determine which analysis provided the earliest reliable prediction of the formation of crystals. Length weighted total counts exhibited similar behavior to unweighted counts. Square weighting of total counts resulted in slightly delayed detection

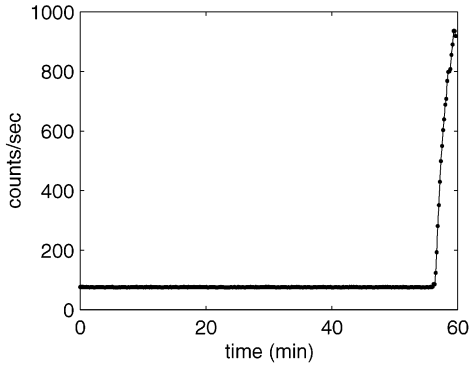

Figure 7. Total counts/s measured over time by FBRM while cooling at 3.7 °C/h in the metastable zone.

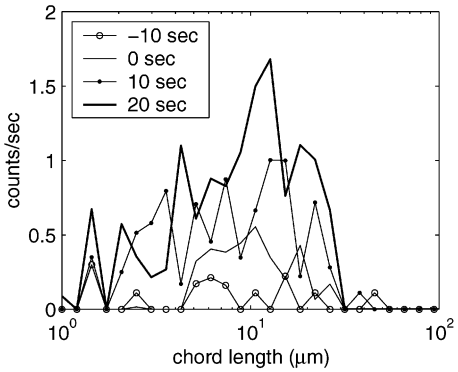

Figure 8. FBRM chord length distribution of nucleated paracetamol crystals (0.020 g/g of water) cooled at 30 °C/h. The first distribution in which the total counts/s increased (and the metastable limit is detected) defines 0 s. The background distribution fluctuates and is shown 10 s before the metastable limit was detected.

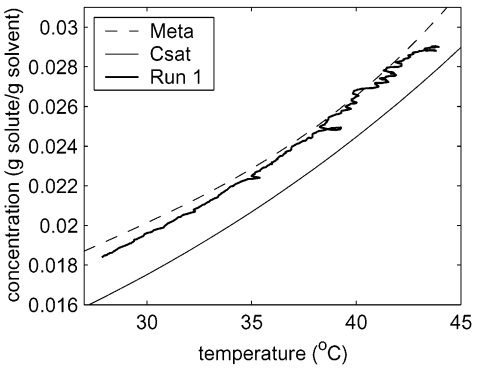

Figure 9. Supersaturation profile followed during seeded batch crystallization which deviates past the metastable limit (run 1) is shown with the solubility curve (—) and the metastable limit for the slow cooling rate (- -).

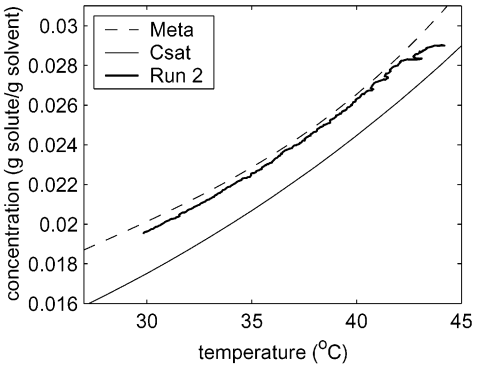

Figure 10. Supersaturation profile followed during seeded batch crystallization which stayed within the metastable limit (run 2) is shown with the solubility curve (—) and metastable limit for the slow cooling rate (- -).

of the metastable limit. Increased noise and/or drift of background signal were observed for 1/length weighting of total counts and for mean chord length with different weightings. Therefore, the temperature where the unweighted total counts/sec increased was taken to be the metastable limit (see Figure 7). The chord length distributions show that nucleated crystals at the metastable limit are around 5−20 μm, and increase over the next 20 s (see Figure 8).

All three methods detected the metastable limit within 0.41 °C of each other for the slow cooling rate. Laser backscattering detected nucleation earliest among the three methods, followed by eye and ATR-FTIR spectroscopy. This is most likely due to its fast sampling interval of 10 s compared to 1 min for the FTIR, and the ability of the FBRM to detect particles smaller than detectable using the naked eye. The difference in the detection ability between the FTIR and laser backscattering is small enough that it can be explained by the difference in sampling time and the sensitivity of the instruments. While the FTIR could be run with a smaller sampling time, this would require fewer scans to be acquired per spectra. The increased noise in the spectra would reduce the accuracy of the solution concentration measurement. For a more soluble system, the sampling time could be reduced.

The determination of the ATR-FTIR calibration curve by chemometrics, the solubility curve by ATR-FTIR spectroscopy, and the metastable limit via ATR-FTIR spectroscopy or laser backscattering can be automated easily using a Visual Basic program that communicates to the FTIR, chemometrics, and laser backscattering software. Such a program was used in this study, with an easy-to-use graphical user interface for carrying out the runs. This automation can increase the reproducibility of the results. The feedback control for the crystallizer, discussed next, was also implemented using a Visual Basic program.

3.4 Supersaturation-Controlled Batch Crystallization. In a significant number of preliminary batch cooling crystallization runs, a large number of agglomerates of paracetamol crystals formed. Preliminary studies indicated that paracetamol crystals smaller than 100 μm were most predominantly involved in agglomeration. Because agglomeration can lead to stability problems with pharmaceuticals, the crystallizer was seeded only with larger paracetamol crystals, and the crystallizer operated to avoid nucleation and agglomeration. A supersaturation profile in the middle of the metastable zone was tried initially (results not shown), but this resulted in a very long batch time due to the slow growth rate of paracetamol. Thus, seeded batch crystallizations of paracetamol were carried out by following a supersaturation profile near the metastable limit of the slow cooling rate to maximize the growth rate while minimizing undesired nucleation.

As shown in Figures 9 and 10, run 1 deviated slightly past the metastable limit while run 2 stayed within the

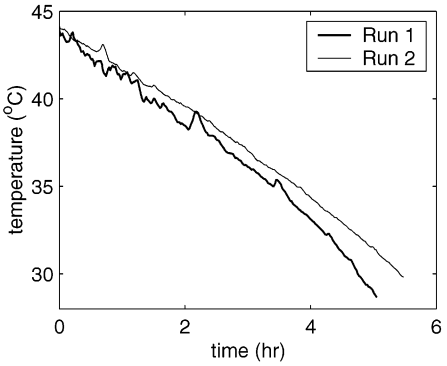

Figure 11. Cooling profiles of supersaturation-controlled seeded batch crystallization for run 1, which deviates past the metastable limit, and for run 2, which stays within the metastable limit.

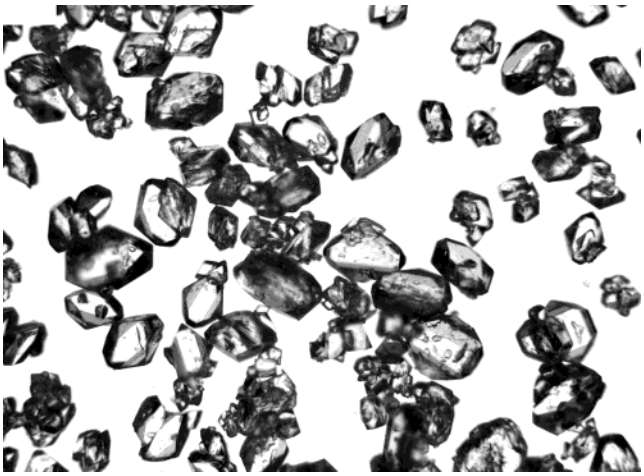

Figure 12. Microscopy image of paracetamol seed crystals used for run 1 (250×).

metastable limit. In both runs, the crystal shape elongated from polyhedral to rectangular, similar to those obtained from low/medium supersaturation (<15%)[5] or slow cooling (3 °C/h).[6] This is not surprising since following the preset supersaturation resulted in cooling profiles with an average cooling rate of about 2.5−3 °C/h (see Figure 11). The crystals produced from run 1 contained agglomerates and crystals of varying sizes (see Figures 12 and 13). The product crystals from run 2 exhibited less agglomeration, and crystals were larger and more uniform in size and shape (see Figures 14 and 15). The chord length distributions showed an increase in total counts in the first 3 h of run 1 indicative of an increase in the number of crystals due to nucleation (see Figure 16) while no appreciable increase in total counts was observed during run 2 (see Figure 17). This suggests that the agglomerates and size variation in the crystals from run 1 are due to nucleation that occurred when supersaturation temporarily exceeded the metastable limit. In run 2, undesired nucleation was avoided by operating within the metastable zone. Since the operating conditions of both runs were similar in the early part of the runs, and there was no initial breeding in run 2, it is unlikely that there was initial breeding in run 1. It seems more likely that the nucleation that occurred when the metastable limit was exceeded was collision breeding or contact nucleation, since this is the dominant secondary nucleation mechanism in most seeded crystallizers.[29,39,40]

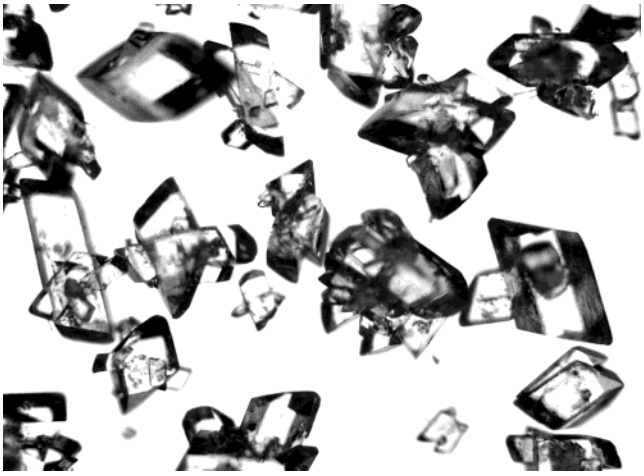

Figure 13. Microscopy image of paracetamol product crystals obtained from run 1 (250×).

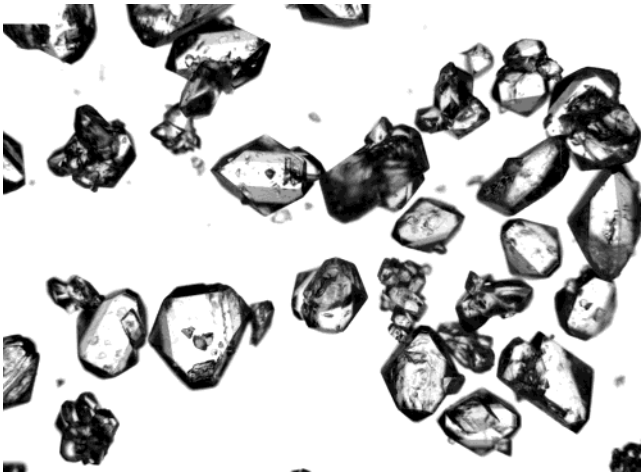

Figure 14. Microscopy image of paracetamol seed crystals used for run 2 (250×).

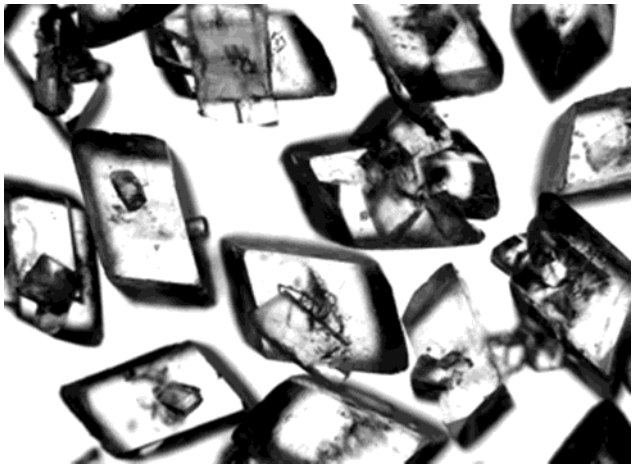

Figure 15. Microscopy image of paracetamol product crystals obtained from run 2 (250×).

Even though the metastable limit was obtained for unseeded nucleation, it is believed that the solution concentration profile was adequate for the seeded system studied here because the obtained metastable limit was near the metastable limit for secondary

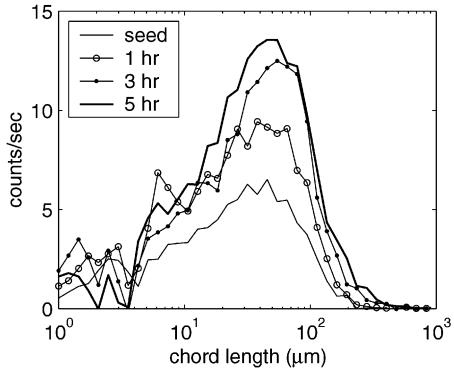

Figure 16. Chord length distributions during run 1.

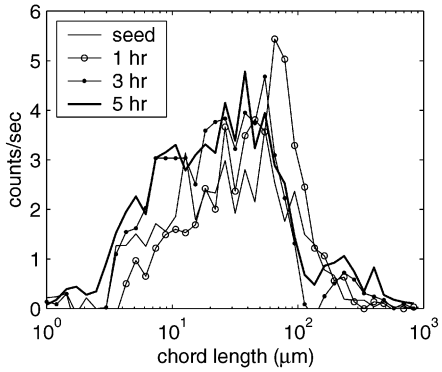

Figure 17. Chord length distributions during run 2.

nucleation. For other systems, it can be important to seed while measuring the metastable limit. Since the metastable limit is known to be sensitive to experimental conditions,[23] it is recommended that a solution concentration profile closer to the solubility curve is followed for industrial systems to ensure acceptably low sensitivity to disturbances.

The crystallization procedure in run 2 provided operating conditions that minimized agglomeration by using the solution concentration as a function of temperature as the setpoint. Lower sensitivity to parameter uncertainties and disturbances may result by using this type of setpoint trajectory instead of the standard temperature trajectory. This method, which includes time only as an implicit variable in the setpoint trajectory, can be used in formulating either open loop or closed loop optimal control design procedures. More research is needed to resolve whether such implicit-in-time optimal control formulations are generally superior to the standard formulation.

3.5 Applicability to Other Systems. Paracetamol in water was selected as the model system because of its low solubility and its tendency to form agglomerates during crystallization. These properties make it especially challenging to measure the characteristics of the particle size distribution and to measure the solution concentration with high enough accuracy for characterizing the kinetics or for on-line control. For a highly soluble system, a smaller sampling time could be used to obtain the same accuracy with ATR-FTIR spectroscopy. Also, more crystals would form during metastability experiments for a highly soluble system. Given the nature of laser backscattering as a "particle counting" technique, for highly soluble systems either a smaller sampling time could be used, or smaller particles could be detected during metastability experiments. Hence the results in this paper can be considered "worst-case". ATR-FTIR spectroscopy and laser backscattering are expected to produce better results for the highly soluble systems normally used in industrial crystallizers.

4. Conclusions

A systematic procedure was developed for identifying the operating conditions for seeded crystallization which minimizes the batch time to obtain large crystals. The procedure was demonstrated with crystallization of paracetamol from water using ATR-FTIR spectroscopy and laser backscattering, which provide in situ measurements of the solution concentration and chord length distribution, respectively. This involved the determination of the metastable zone (solubility curve and metastable limit) and the operation of supersaturation-controlled seeded batch crystallization. Among the different methods used for detecting the onset of nucleation, laser backscattering was more sensitive in detecting the metastable limit compared to ATR-FTIR and visual observation. It was shown that laser backscattering could be used to measure the metastable limit for agglomerating systems, and to characterize the size distribution that forms after passing the metastable limit. In seeded batch crystallization, large paracetamol crystals were produced by controlling the concentration in situ near the metastable limit using ATR-FTIR. An appropriately seeded crystallizer controlled within the metastable zone resulted in negligible nucleation and agglomeration, and exhibited consistent growth of large crystals.

Acknowledgment. Support from Merck and DuPont is acknowledged.

References

(1) Chow, A. H.-L.; Chow, P. K. K.; Zhongshan, W.; Grant, D. J. W. *Int. J. Pharm.* **1985**, *24*, 239−258.
(2) Green, D. A.; Meenan, P. In *Crystal Growth of Organic Materials*; Myerson, A. S., Green, D. A., Meenan, P., Eds.; American Chemical Society: Washington, DC, 1995; pp 78−84.
(3) Shekunov, B. Y.; Aulton, M. E.; Adama-Acquah, R. W.; Grant, D. J. W. *J. Chem. Soc., Faraday Trans.* **1996**, *92*, 439−444.
(4) Shekunov, B. Y.; Grant, D. J. W. *J. Phys. Chem. B* **1997**, *101*, 3973−3979.
(5) Ristic, R. I.; Finnie, S.; Sheen, D. B.; Sherwood, J. N. *J. Phys. Chem. B* **2001**, *105*, 9057−9066.
(6) Granberg, R. A.; Bloch, D. C.; Rasmuson, A. C. *J. Cryst. Growth* **1999**, *198/199*, 1287−1293.
(7) Granberg, R. A.; Ducreux, C.; Gracin, S.; Rasmuson, A. C. *Chem. Eng. Sci.* **2001**, *56*, 2305−2313.
(8) Hendriksen, B. A.; Grant, D. J. W. *J. Cryst. Growth* **1995**, *156*, 252−260.
(9) Liu, X. Y. *App. Phys. Lett.* **2001**, *79*, 39−41.
(10) Liu, X. Y. *J. Phys. Chem. B* **2001**, *105*, 11550−11558.
(11) Mullin, J. W. In *Crystal Growth*; Pamplin, B. R., Ed.; Pergamon Press: New York, 1980; pp 521−565.
(12) Rawlings, J. B.; Miller, S. M.; Witkowski, W. R. *Ind. Eng. Chem. Res.* **1993**, *32*, 1275−1296.
(13) Braatz, R. D. *Annu. Rev. Control* **2002**, *26*, in press.
(14) Dunuwila, D. D.; Carroll II, L. B.; Berglund, K. A. *J. Cryst. Growth* **1994**, *137*, 561−568.
(15) Dunuwila, D. D.; Berglund, K. A. *J. Cryst. Growth* **1997**, *179*, 185−193.

(16) Wang, F.; Berglund, K. A. *Ind. End. Chem. Res.* **2000**, *39*, 2101−2104.
(17) Groen, H.; Roberts, K. J. *Anal. Chim. Acta* **2001**, *105*, 10723−10730.
(18) Lewiner, F.; Klein, J. P.; Puel, F.; Fevotte, G. *Chem. Eng. Sci.* **2001**, *56*, 2069−2084.
(19) Lewiner, F.; Fevotte, G.; Klein, J. P.; Puel, F. *J. Cryst. Growth* **2001**, *226*, 348−362.
(20) Togkalidou, T.; Fujiwara, M.; Patel, S.; Braatz, R. D. *J. Cryst. Growth* **2001**, *231*, 534−543.
(21) Togkalidou, T.; Tung, H.-H.; Sun, Y.; Andrews, A.; Braatz, R. D. *Org. Proc. Res. Dev.* **2002**, *6*, 317−322.
(22) Eek, R. Ph.D. Thesis, Delft University of Technology, The Netherlands, 1995.
(23) Nyvlt, J.; Sohnel, O.; Matuchova, M.; Broul, M. *The Kinetics of Industrial Crystallization*; Elsevier: New York, 1985.
(24) Singh, B. *Anal. Proc.* **1993**, *30*, 495−496.
(25) Tahti, T.; Louhi-Kultanen, M.; Palosaari, S. In *Int. Symp. Ind. Cryst., 14th*; Institution of Chemical Engineers: Rugby, UK, 1999; pp 1−9.
(26) Miller, S. M.; Rawlings, J. B. *AIChE J.* **1994**, *40*, 1312−1327.
(27) Gunawan, R.; Ma, D. L.; Fujiwara, M.; Braatz, R. D. *Int. J. Mod. Phys. B* **2002**, *16*, 367−374.
(28) Braatz, R. D.; Hasebe, S. In *Chemical Process Control VI*; Rawlings, J. B., Ogunnaike, B. A., Eds.; AIChE Press: New York, 2002.
(29) Gutwald, T.; Mersmann, A. *Chem. Eng. Technol.* **1990**, *13*, 229−237.
(30) Braatz, R. D. In *The Control Handbook*; Levine, W. S., Ed.; CRC Press: Boca Raton, Florida, 1995; pp 215−224.31.
(31) Morari, M.; Zafiriou, E. *Robust Process Control*; Prentice Hall: Englewood Cliffs, New Jersey, 1989.
(32) Workman, J. J.; Mobley, P. R.; Kowalski, B. R.; Bro, R. *Appl. Spec. Rev.* **1996**, *31*, 73−124.
(33) Mobley, P. R.; Kowalski, B. R.; Workman, J. J.; Bro, R. *Appl. Spec. Rev.* **1996**, *31*, 347−368.
(34) Bro, R.; Workman, J. J.; Mobley, P. R.; Kowalski, B. R. *Appl. Spec. Rev.* **1997**, *32*, 237−261.
(35) Ramos, M. L.; Tyson, J. F.; Curran, D. J. *Anal. Chim. Acta* **1998**, *364*, 107−116.
(36) Xie, Y.; Kalivas, J. *Anal. Chim. Acta* **1997**, *348*, 19−27.
(37) Grant, D. J. W.; Mehdizadeh, M.; Chow, A. H.-L.; Fairbrother, J. E. *Int. J. Pharm.* **1984**, *18*, 25−33.
(38) Granberg, R. A.; Rasmuson, A. C. *J. Chem. Eng. Data* **1999**, *44*, 4, 1391−1395.
(39) Ottens, E. P. K.; Janse, A. H.; De Jong, E. J. *J. Cryst. Growth*, **1972**, *13/14*, 500−505.
(40) Myerson, A. S.; Ginde, R. In *Handbook of Industrial Crystallization*; Myerson, A. S., Ed.; Butterworth-Heinemann: Boston, 1993; p 46.

CG0200098